Available online at www.sciencedirect.com

ScienceDirect

Procedia Structural Integrity 19 (2019) 617–626

Structural Integrity Procedia

www.elsevier.com/locate/procedia

Fatigue Design 2019

The Peak Stress Method combined with 3D finite element models to assess the fatigue strength of complex welded structures

Alberto Campagnolo[a], Ilaria Roveda[a], Giovanni Meneghetti[a]*,

[a] *University of Padova, Department of Industrial Engineering, Via Venezia 1, 35131 Padova, Italy*

Abstract

The Peak Stress Method (PSM) is a rapid and engineering application of the notch stress intensity factor (NSIF) approach for the fatigue strength assessment of welded structures, which employs the singular linear elastic peak stresses calculated by FEM using coarse meshes. First, the PSM was calibrated to rapidly estimate the NSIFs by adopting 3D, eight-node brick elements and by using the submodeling technique. Given the increasing 3D modelling of large and complex structures in the industry, the application of the PSM combined with 3D FE models has recently been speeded up by calibrating ten-node tetra elements, which allow to directly discretize complex 3D geometries making submodeling unnecessary. In the present contribution, the PSM has been calibrated by analysing several 3D mode I, II and III V-notch problems, by adopting either four-node or ten-node tetra elements. In particular, the 3D PSM with ten-node tetra elements has been extended to V-notch opening angles that had not been taken into account in a previous calibration, namely (i) 120° under mode I and (ii) 90° and 120° under mode III loadings. Then, an applicative example has been considered, which is relevant to a large-scale and rather complex steel welded structure, having overall size on the order of meters. The mesh density requirements to apply the PSM to the considered large-scale welded structure using either four-node tetra elements or ten-node tetra elements have been compared in order to assess the solution time required by the two types of FE meshes.

Peer-review under responsibility of the Fatigue Design 2019 Organizers.

Keywords: Notch Stress Intensity Factor; Peak Stress Method; Coarse Mesh; Welded joints; Fatigue

* Corresponding author. Tel.: +39 049 8276751; fax: +39 049 8276785.
E-mail address: giovanni.meneghetti@unipd.it

2452-3216
Peer-review under responsibility of the Fatigue Design 2019 Organizers.
10.1016/j.prostr.2019.12.067

1. Introduction

The singular linear elastic stress fields close to a sharp V-notch tip, see an example in Fig. 1a, can be expressed as functions of the notch stress intensity factors (NSIFs), which quantify the intensity of the local stress components. The stress singularities related to sharp notches under mode I (opening) and mode II (sliding) loadings were studied by Williams (1952), while Qian and Hasebe (1997) analysed the notch problem under mode III (tearing) loading. The mode I, II and III NSIFs can be defined according to Gross and Mendelson (1972) on the basis of the following equation:

$$K_i = \sqrt{2\pi} \cdot \lim_{r \to 0} \left[\left(\sigma_{jk} \right)_{\theta=0} \cdot r^{1-\lambda_i} \right] \quad \text{where} \quad i=1,2,3 \quad \text{and} \quad \sigma_{jk} = \sigma_{\theta\theta}, \tau_{r\theta}, \tau_{\theta z} \ \text{respectively} \tag{1}$$

where λ_1, λ_2 and λ_3 represent the mode I, II and III eigenvalues, respectively, which are dependent on the opening angle 2α (Williams 1952; Qian and Hasebe 1997), while $\sigma_{\theta\theta}$, $\tau_{r\theta}$ and $\tau_{\theta z}$ are the local stress components calculated along the notch bisector line, i.e. at $\theta=0$ according to Fig. 1a.

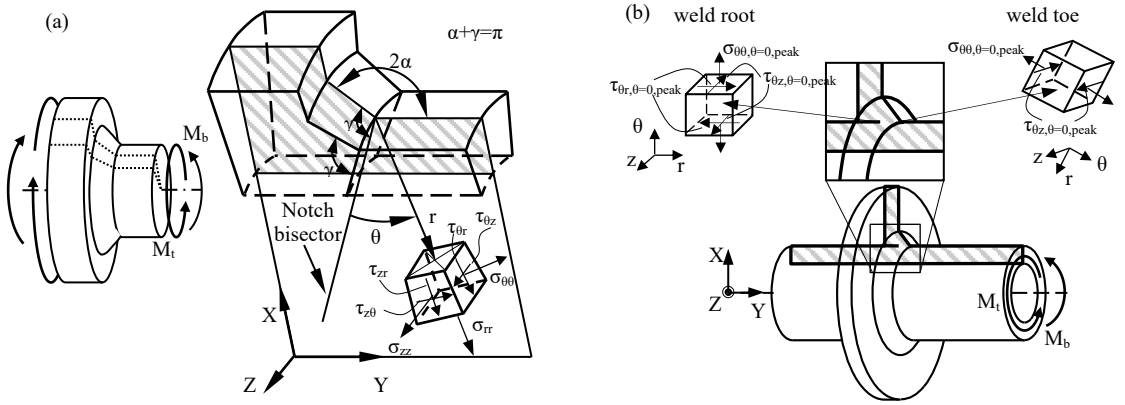

Fig 1: (a) Polar reference system centred at the weld toe of a typical tube-to-flange welded joint geometry subjected to multiaxial bending and torsion loading. (b) Sharp V-shaped notches in a welded joint at the weld root (2α= 0°) and at the weld toe (2α typically equal to 135°). Definition of peak stresses $\sigma_{\theta\theta,\theta=0,peak}$, $\tau_{r\theta,\theta=0,peak}$ and $\tau_{\theta z,\theta=0,peak}$.

The NSIF-based approach has been adopted in the literature for the fatigue strength assessment of sharply notched components (Kihara and Yoshii 1991). Dealing with welded structures, NSIFs have been employed to correlate the fatigue strength under uniaxial (Lazzarin and Tovo 1998; Atzori and Meneghetti 2001) as well as multiaxial loadings (Lazzarin et al. 2004). However, it is worth noting that the evaluation of NSIF-parameters by post-processing the numerical results of FE analyses presents a major drawback in engineering applications, very refined FE meshes (element size on the order of 10^{-5} mm) being necessary to calculate the NSIFs on the basis of definition (1). In the case of three-dimensional complex and large-scale structures, the solution of the FE model as well as the post-processing task could be even more time-consuming.

A FE-oriented, rapid technique, namely the Peak Stress Method (PSM), has been proposed to speed up the application of the NSIF-based approach by means of FE analyses with coarse meshes, the element size being some orders of magnitude larger than that necessary to apply definition (1). Another advantage of the PSM is that it requires only a single stress value to estimate the NSIFs, instead of a number of *stress-distance* numerical data, as required to apply definition (1). The PSM allows a rapid estimation of the NSIF relevant to sharp and open V-notches under mode I (Meneghetti and Lazzarin 2007; Meneghetti and Guzzella 2014), the SIF of cracks under mode II (Meneghetti 2012) and the NSIF of open V-notches under mode III (Meneghetti 2013). It should be noted that any NSIF-based local approach for the structural strength assessment can in principle be reformulated taking advantage of the PSM. As an example, the PSM has been adopted in combination with the averaged strain energy density (SED) approach to estimate the fatigue life of welded joints under axial (Meneghetti and Lazzarin 2011; Meneghetti 2012), torsion (Meneghetti 2013) and multiaxial (Meneghetti et al. 2017a; Meneghetti et al. 2017b) loading conditions.

Essentially, the PSM allows to rapidly estimate the NSIF-parameters K_1, K_2 and K_3 by employing the singular, linear elastic, opening (mode I), sliding (mode II) and tearing (mode III) peak stresses $\sigma_{\theta\theta,\theta=0,peak}$, $\tau_{r\theta,\theta=0,peak}$ and

$\tau_{\theta z,\theta=0,peak}$, respectively, which are referred to the V-notch bisector line, according to Fig. 1b, and calculated at the V-notch tip from FE analyses with coarse meshes. The NSIFs can be estimated according to PSM by applying the following expressions (Meneghetti and Lazzarin 2007; Meneghetti 2012; Meneghetti 2013):

$$K_1 \cong K^{*}_{FE} \cdot \sigma_{\theta\theta,\theta=0,peak} \cdot d^{1-\lambda_1} \quad (2a) \qquad K_2 \cong K^{**}_{FE} \cdot \tau_{r\theta,\theta=0,peak} \cdot d^{0.5} \quad (2b) \qquad K_3 \cong K^{***}_{FE} \cdot \tau_{\theta z,\theta=0,peak} \cdot d^{1-\lambda_3} \quad (2c)$$

where *d* represents the 'global element size', i.e. the average FE size given as input parameter to the free mesh generation algorithm of the numerical code, while coefficients K^{*}_{FE}, K^{**}_{FE} and K^{***}_{FE} depend on the calibration options: (i) element type and formulation; (ii) mesh pattern of finite elements and (iii) procedure to extrapolate stresses at FE nodes, as it has been discussed in detail in (Meneghetti et al. 2018).

Originally, the coefficients K^{*}_{FE}, K^{**}_{FE} and K^{***}_{FE} have been calibrated by employing 2D, four-node plane quadrilateral elements of Ansys® element library (Meneghetti and Lazzarin 2007; Meneghetti 2012; Meneghetti 2013) and resulted equal to 1.38, 3.38 and 1.93, respectively, such values being valid under the conditions discussed in the relevant literature (Meneghetti and Lazzarin 2007; Meneghetti 2012; Meneghetti 2013; Meneghetti and Guzzella 2014), to which the reader is referred. In the context of a Round Robin between Italian Universities, K^{*}_{FE} and K^{**}_{FE} have been also calibrated for six commercial FE codes other than Ansys® (Meneghetti et al. 2018). Then, the PSM has been extended to be applied in combination with 3D, eight-node brick elements (Meneghetti and Guzzella 2014), by employing the submodeling technique available in Ansys® code. More in detail, when analysing a complex 3D welded structure a submodel consisting of brick elements must be defined after having analysed a main model meshed with ten-node tetra elements.

Given the increasing adoption of 3D modelling of large and complex structures in industrial applications, the 3D PSM has recently been speeded up by calibrating ten-node tetra elements (Campagnolo and Meneghetti 2018), which allow to discretize complex 3D geometries and to apply the PSM to the results of a single analysis, making submodeling unnecessary. In the present contribution, parameters K^{*}_{FE}, K^{**}_{FE} and K^{***}_{FE} have been calibrated by analysing several 3D mode I, II and III notch problems, by adopting either four-node or ten-node tetra elements. In particular, the PSM combined with ten-node tetra elements has been extended to V-notch opening angles that had not been taken into account in a previous calibration (Campagnolo and Meneghetti 2018), namely 120° under mode I and 90° and 120° under mode III loadings. Afterwards, the minimum mesh density requirements derived for four-node and for ten-node tetra elements have been compared in the case of a large-scale and rather complex steel welded structure, having overall size on the order of meters and containing several different welded details.

2. Calibrating the PSM with tetra elements

In FE analyses of 3D notched structures using tetrahedral elements, it has been argued (Campagnolo and Meneghetti 2018) that the mesh pattern obtained by the free mesh generation algorithm is intrinsically irregular, which means that the nodes located at the notch tip could be shared by a different number of elements having significantly different shape and size (the FE size *d* given as input being an average value). Accordingly, the peak stress could vary along the notch tip profile even in the case of a constant applied NSIF. The variability of the peak stress along the notch tip profile can be reduced by introducing an average peak stress value, which has been defined in (Campagnolo and Meneghetti 2018) as the moving average on three adjacent vertex nodes, i.e. at the generic node n=k:

$$\overline{\sigma}_{ij,peak,n=k} = \left. \frac{\sigma_{ij,peak,n=k-1} + \sigma_{ij,peak,n=k} + \sigma_{ij,peak,n=k+1}}{3} \right|_{n=node} \quad (3)$$

Taking advantage of definition (3), the PSM combined with tetra elements has been calibrated by analysing several 3D notch problems under pure mode I, pure mode II and pure mode III loadings. Once evaluated the average peak stresses from Eq. (3), the coefficients K^{*}_{FE}, K^{**}_{FE} and K^{***}_{FE} have been calculated by re-arranging Eqs. (2a)-(2c) in the following fashion:

$$K^{*}_{FE} \cong \frac{K_1}{\overline{\sigma}_{\theta\theta,\theta=0,peak} \cdot d^{1-\lambda_1}} \quad (4a) \qquad K^{**}_{FE} \cong \frac{K_2}{\overline{\tau}_{r\theta,\theta=0,peak} \cdot d^{0.5}} \quad (4b) \qquad K^{***}_{FE} \cong \frac{K_3}{\overline{\tau}_{\theta z,\theta=0,peak} \cdot d^{1-\lambda_3}} \quad (4c)$$

All FE analyses adopted the same material properties, namely a structural steel with Young's modulus equal to

206000 MPa and a Poisson's ratio ν of 0.3.

Either 3D, four-node, linear tetrahedral elements (SOLID 285 of Ansys® element library) or 3D, ten-node, quadratic tetrahedral elements (SOLID 187 of Ansys® element library) have been used in the FE analyses. Both elements had 4 Gauss points, being the sole element formulation available in Ansys®. It should be noted that only peak stresses calculated at vertex nodes of tetra elements have to be introduced in Eq. (3); therefore, when ten-node, quadratic tetra elements are adopted, stresses at mid-side nodes – even though located at the notch tip - must be neglected. It might be useful to recall that stresses at mid-side nodes are provided by Ansys code® when "path operations" or "GET commands" are used in the post-processing environment; by contrast, they are automatically excluded by adopting "list nodal results" or "query results" in post-processing. After having selected the proper element type, the global element size *d* has been the sole parameter given as input to the free mesh generation algorithm available in Ansys.

Concerning mode I and mode II notch problems, to obtain a uniform distribution of the relevant NSIFs along the notch tip profile, plane-strain conditions have been simulated in the FE analyses by constraining the out-of-plane element displacement u_z (and therefore the corresponding ε_z strain component results $\varepsilon_z = 0$).

2.1. 3D problems (plane strain), mode I loading, $0° \le 2\alpha \le 135°$

Several three-dimensional notch and crack problems under pure mode I (see Fig. 2(a), (b), (c) and (d)) have been analysed, by varying the characteristic size of the notch problem *a* in the range between 1 and 50 mm and considering four values of the notch opening angle, i.e. $2\alpha = 0°$, 90°, 120° and 135°, 0° and 135° being typical for weld root and toe profiles, respectively. 3D linear elastic FE analyses have been carried out by simulating plane strain conditions and by adopting either four node or ten-node tetra elements to calculate the peak stresses. Only one eighth of each geometry has been analysed taking advantage of the triple symmetry condition. The free mesh has been generated after providing the average element size *d* to the automatic generation algorithm available in Ansys. This task is accomplished by using the 'global element size' input parameter. A mesh density ratio *a/d* in the range between 1 and 13 has been explored, by varying either the notch size *a* or the element size *d*. A nominal gross-section stress equal to 1 MPa has been applied to each FE model. Once solved the FE model, the opening peak stress $\sigma_{11,peak}$, which was almost equal to $\sigma_{\theta\theta,\theta=0,peak}$ in all cases of Figs. 2(a)-(d), has been calculated at vertex nodes located at the notch or crack tip lines; afterwards, Eq. (3) has been adopted to evaluate the average peak stress at each vertex node.

2.2. 3D problems (plane strain), mode II loading, $2\alpha=0°$

A plate having the geometry shown in Fig. 2(e), weakened by a central crack ($2\alpha = 0°$) and subjected to pure mode II loading has been analysed by varying the crack length in the range $6 \le 2a \le 200$ mm. 3D linear elastic FE analyses have been performed by simulating plane strain conditions and by using either four node or ten-node tetra elements to calculate the peak stresses. The mesh density ratio *a/d* has been varied in the range from 1 to 20. Only one eighth of the geometry has been analysed taking advantage of the double anti-symmetry on planes Y-Z and X-Z and the symmetry on plane X-Y. The pure mode II loading has been applied by means of displacements $u_x=u_y=1.262\cdot10^{-3}$ mm at the plate free faces, corresponding to a nominal gross shear stress of 1 MPa when crack is absent. Once solved the FE model, the sliding peak stress $\tau_{r\theta,\theta=0,peak} = \tau_{xy,peak}$ has been calculated at the vertex nodes located at the crack tip profile, afterwards Eq. (3) has been used to evaluate the average peak stress at each vertex node.

2.3. 3D problems, mode III loading, $0° \le 2\alpha \le 135°$

The three-dimensional notch and crack problems under pure mode III reported in Fig. 2(f), (g) and (h), have been analysed by varying the notch size *a* in the range between 2 and 15 mm and by considering four values of the notch opening angle, i.e. $2\alpha = 0°$, 90°, 120° and 135°. 3D linear elastic FE analyses have been performed by adopting either four node or ten-node tetra elements to calculate the peak stress values. The mesh density ratio *a/d* has been varied in the range from 1 to 10. A nominal gross shear stress equal to 1 MPa has been applied to each FE model. After having solved the FE model, the tearing peak stress $\tau_{\theta z,\theta=0,peak}$ has been calculated at the vertex nodes located at the notch tip line by adopting a local coordinate system r-θ-z rotated at each node as shown in Fig. 1b. Afterwards, Eq. (3) has been adopted to evaluate the average peak stress at each vertex node.

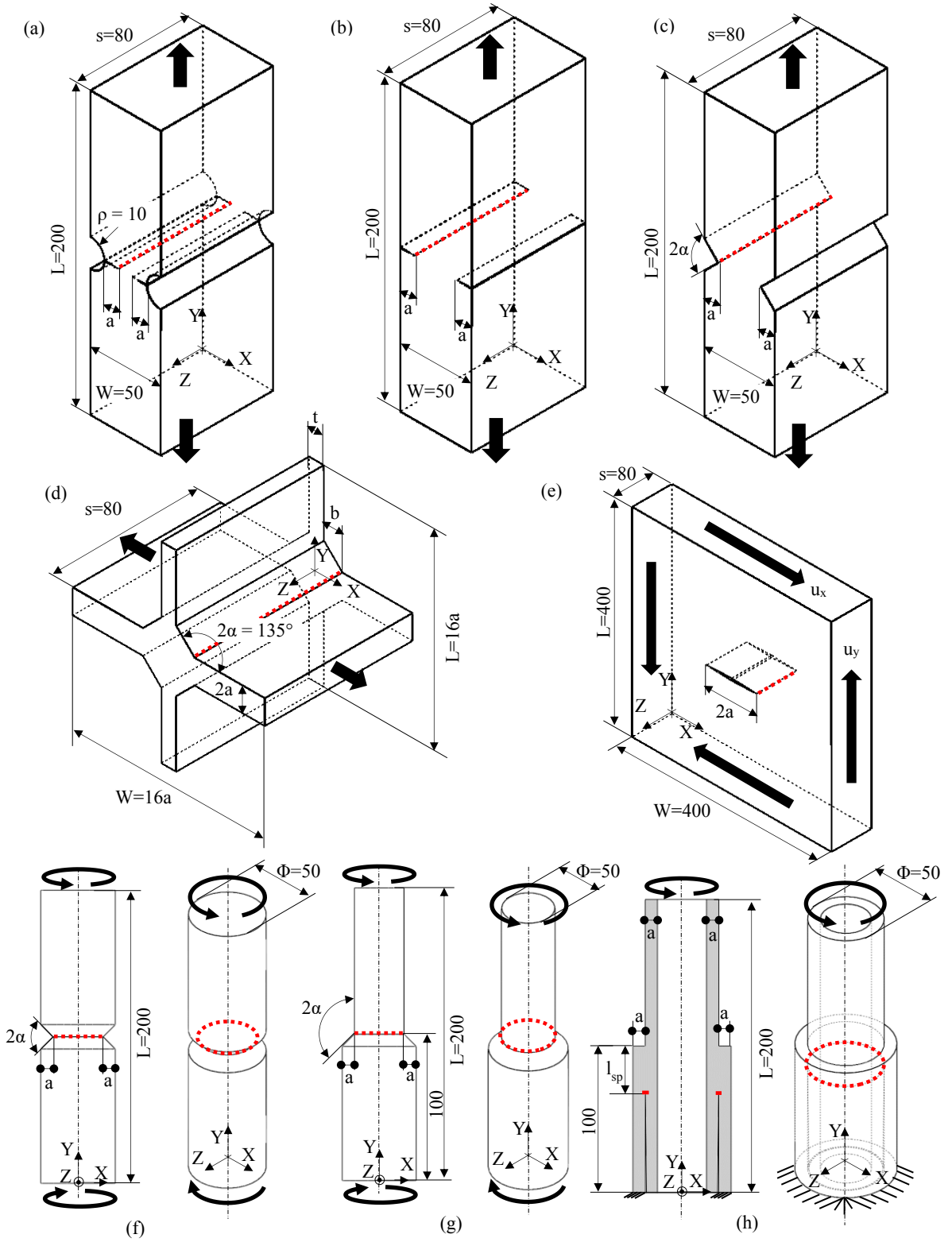

Fig. 2. Geometries of 3D notch problems: (a), (b), (c), (d) under mode I loading; (e) under mode II loading; (f), (g), (h) under mode III loading. Red lines indicate the analysed cracks and notch tips.

For all geometries of Fig. 2, the exact values of the relevant NSIFs, namely K_1, K_2 and K_3, to be input in Eq. (4a)-(4c), respectively, have been evaluated from definition (1) applied to the stress-distance numerical results calculated by means of 2D FE analyses with very refined meshes (the size of the smallest element being on the order of 10^{-5} mm). Concerning geometries under mode I and mode II loadings, eight-node, quadratic quadrilateral elements (PLANE 183 of Ansys® element library) under plane strain conditions have been employed, while dealing with geometries under mode III loading, eight-node, quadratic quadrilateral harmonic elements (PLANE 83 of Ansys® element library) have been used.

3. Results of FE analyses

Figures 3 and 4 report the PSM-parameters K^*_{FE}, K^{**}_{FE} and K^{***}_{FE} evaluated from Eqs. (4a)-(4c) by adopting either four-node tetra elements or ten-node tetra elements, respectively, as functions of the mesh density ratio *a/d*. It is worth noting that in each numerical analysis, coefficients K^*_{FE}, K^{**}_{FE} and K^{***}_{FE} showed a non-uniform distribution along the notch or crack tip lines, due to the variability of the average peak stress. Accordingly, Figs. 3 and 4 report the average value of the PSM-parameters K_{FE} calculated from each FE analysis along with the relevant bar, representing the range between minimum and maximum K_{FE} values calculated along the notch or crack tip lines.

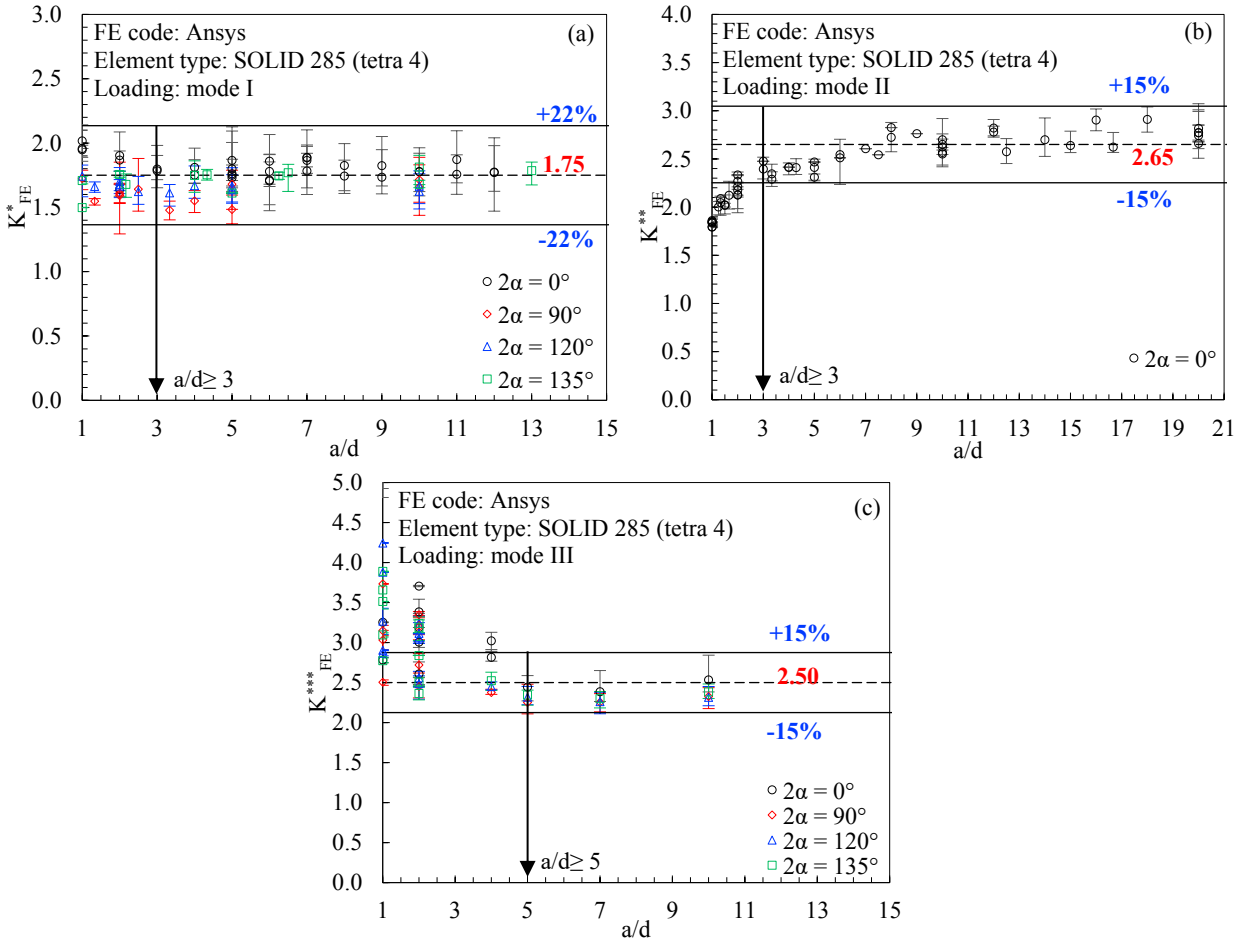

Fig. 3. Calibration of PSM combined with 4-node tetrahedral elements: (a) K^*_{FE} (Eq. 4a), (b) K^{**}_{FE} (Eq. 4b), (c) K^{***}_{FE} (Eq. 4c).

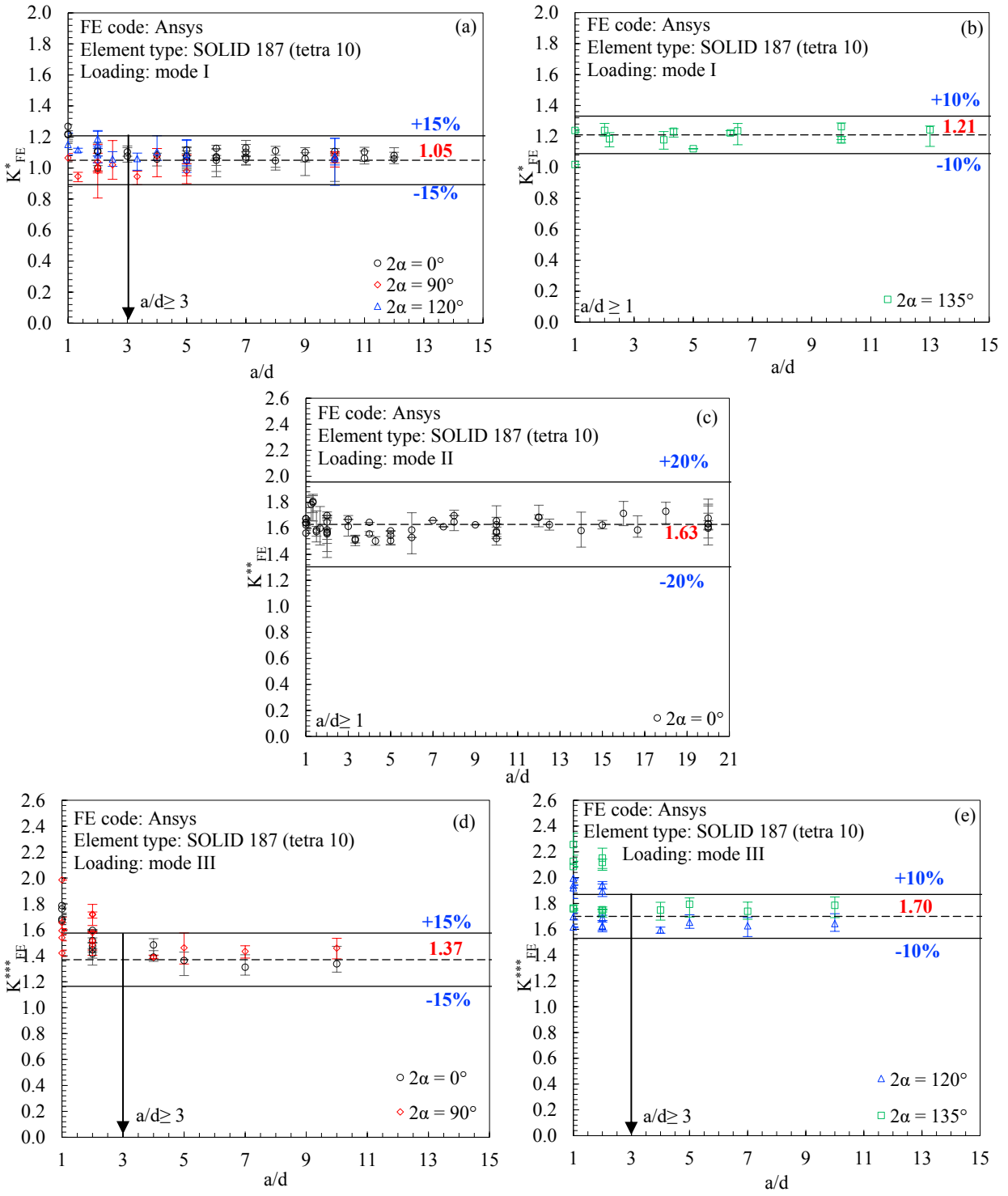

Fig. 4. Calibration of PSM combined with 10-node tetrahedral elements: K^{*}_{FE} (Eq. 4a) for (a) 2α = 0°, 90° and 120°, (b) 2α = 135°; (c) K^{**}_{FE} (Eq. 4b) for 2α = 0°; K^{***}_{FE} (Eq. 4c) for (d) 2α = 0° and 90°, (e) 2α = 120° and 135°.

Concerning 3D, four-node, linear tetra elements (SOLID 285 of Ansys® element library), Fig. 3 shows that:

- Under mode I loading (see Fig. 3a), $K^{*}_{FE} \cong 1.75 \pm 22\%$ for all considered values of the notch opening angle 2α. Convergence is obtained when $a/d \geq 3$.
- Dealing with mode II loading (see Fig. 3b), $K^{**}_{FE} \cong 2.65 \pm 15\%$ and convergence is obtained when the ratio $a/d \geq 3$.
- Concerning mode III loading, the obtained results are reported in Fig. 3c, which shows that $K^{***}_{FE} \cong 2.50 \pm 15\%$ for any notch opening angle 2α. Convergence is obtained when $a/d \geq 5$.

Dealing with 3D, ten-node, quadratic tetra elements (SOLID 187 of Ansys® element library), Fig. 4 shows that:

- Under mode I loading, Figs. 4a and b show that $K^{*}_{FE} \cong 1.05 \pm 15\%$ for 2α equal to 0°, 90° or 120°, while $K^{*}_{FE} \cong 1.21 \pm 10\%$ when 2α equals 135°. Convergence is obtained when $a/d \geq 3$ for 2α equal to 0°, 90° or 120° and 1 for 2α equal to 135°.
- Concerning with mode II loading (see Fig. 4c), $K^{**}_{FE} \cong 1.63 \pm 20\%$, while convergence is obtained for a ratio $a/d \geq 1$.
- Dealing with mode III loading, the obtained results are reported in Figs. 4d and e, which show that $K^{***}_{FE} \cong 1.37 \pm 15\%$ for 2α equal to 0° or 90°, while $K^{***}_{FE} \cong 1.70 \pm 10\%$ for 2α equal to 120° or 135°. Convergence is obtained when $a/d \geq 3$ for all considered notch opening angles 2α.

It is worth noting that in the case of ten-node, quadratic tetrahedral elements, the results obtained here are in agreement with previous calibration reported in (Campagnolo and Meneghetti 2018). The parameters K^{*}_{FE} and K^{***}_{FE} have slightly been modified to include other notch opening angles, namely 120° under mode I on one side, and 90° as well as 120° under mode III on the other side.

A summary of the calibration of PSM with either four-node or ten-node tetra elements is reported in Table 1.

Table 1. Summary of calibration of K^{*}_{FE}, K^{**}_{FE} and K^{***}_{FE} for tetra elements of Ansys® element library.

2α [°]	Mode I				Mode II				Mode III			
	Tetra 4		Tetra 10		Tetra 4		Tetra 10		Tetra 4		Tetra 10	
	K^{*}_{FE}	$(a/d)_{min}$	K^{*}_{FE}	$(a/d)_{min}$	K^{**}_{FE}	$(a/d)_{min}$	K^{**}_{FE}	$(a/d)_{min}$	K^{***}_{FE}	$(a/d)_{min}$	K^{***}_{FE}	$(a/d)_{min}$
0	1.75 ± 22%	3	1.05 ± 15%	3	2.65 ± 15%	3	1.63 ± 20%	1	2.50 ± 15%	5	1.37 ± 15%	3
90					-	-	-	-				
120											1.70 ± 10%	3
135			1.21 ± 10%	1								

4. Application to a case study

After having calibrated the three-dimensional PSM combined with tetra elements, the applicative example shown in Fig. 5a has been considered, which is a large-scale welded steel structure consisting of a sluice gate having overall size on the order of tens of meters. The considered detail has size on the order of meters and it has been previously analysed by adopting the 3D PSM based on ten-node tetra elements and High Performance Computing (HPC) to run the analysis (Campagnolo and Meneghetti 2018). The detail of Fig. 5a includes many different welded geometries, including T- and cruciform, fillet- as well as full-penetration welded joints, with plate thicknesses in the range between 10 mm and 58 mm.

Weld toes and weld roots of the detail shown in Fig. 5a are mainly subjected to mode I loading, with mode II and mode III stresses being active only in a limited number of welded regions. To estimate the NSIFs using the 3D PSM based on tetra elements, the minimum mesh density ratios reported in Table 1 must be guaranteed:

- By considering for a while the weld toe and the weld root under mode I loading only, the mesh density ratio a/d must be greater than 3 to adopt either four-node or ten-node tetra elements. The minimum plate thickness being equal to $2a = 10$ mm, the mesh density ratio $a/d = 3$ corresponds to $d = 1.66$ mm. It is evident that using four-node tetra elements would be advantageous as compared to ten-node tetra elements, because for the same

mesh density four-node tetra elements generate less than half nodes as compared to ten-node tetra elements. It could be verified that the number of degrees of freedom (dof) of the FE model (FE nodes x degrees of freedom per node) is equal to 20 millions when adopting four-node tetra elements against 140 millions when adopting ten-node tetra elements; the advantage gained by reducing the solution time is clearly appreciable.

- By considering the actual design situation, where the weld toe and the weld root undergo a general mixed mode I+II+III loading, the mesh density ratio *a/d* must be greater than 5 and 3 for four-node and ten-node tetra elements, respectively. Again, since 2*a* = 10 mm, therefore *a/d* = 5 corresponds to *d* = 1 mm (see Fig. 5b), while *a/d* = 3 means *d* = 1.66 mm (see Fig. 5c). It could be verified that even if the four-node tetra element mesh is more refined than the ten-node mesh, the number of degrees of freedom (dof) is equal to 60 millions in the former case, while it is 140 millions in the latter case. Therefore, the use of four-node tetra elements is still advantageous. While the comparison of NSIFs obtained with four-node and ten-node tetra element meshes for the structure reported in Fig. 5 will be performed in the future, in a previous analysis (Campagnolo and Meneghetti 2018) it was found that the ten-node tetra element mesh provides NSIFs values in fair agreement with those calculated using a shell-to-solid FE technique (Colussi et al. 2017), the maximum deviation between results obtained with the two method being 10% at the toe side and 15% at the root side.

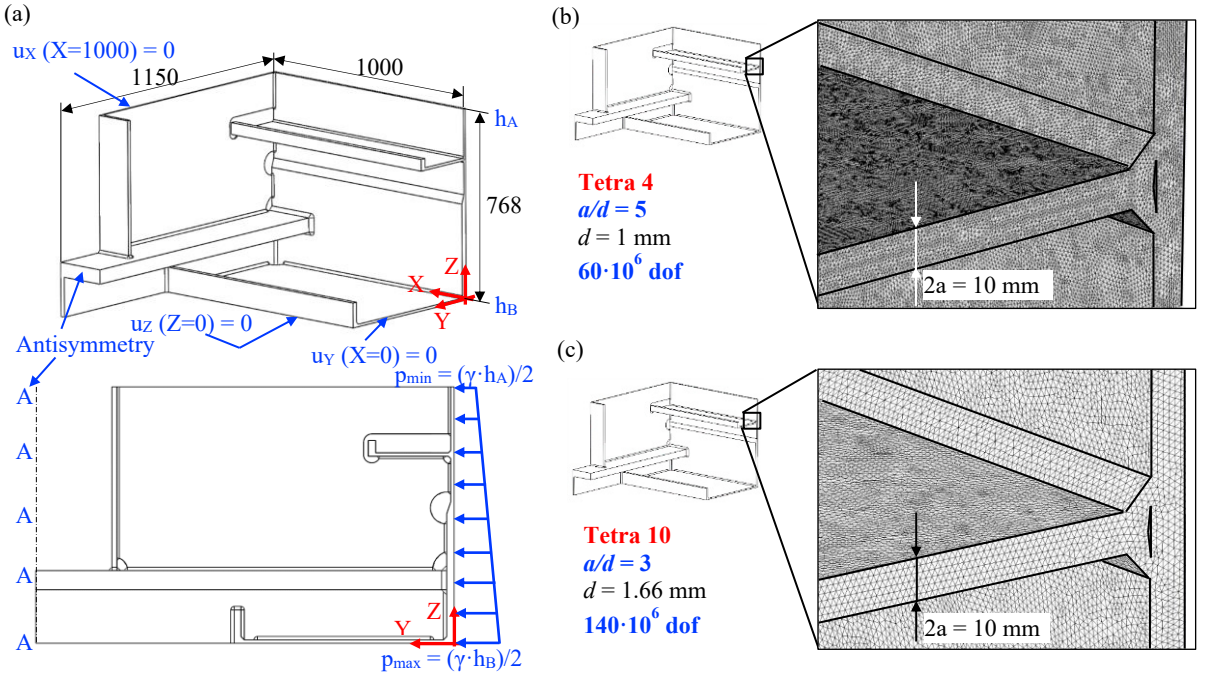

Fig. 5. (a) Geometry (dimensions are in mm) and boundary conditions applied to the detail of the sluice gate. γ is the water specific weight, h_A and h_B are the geodetic height referred to the free surface and are equal to 9.232 m and 10 m, respectively. Coarse meshes generated in Ansys environment to analyse weld toe and weld root under a general mode I+II+III loading condition by adopting (b) four-node tetra elements with a/d = 5 and (c) ten-node tetra elements with a/d = 3 according to Table 1. Dof = degree of freedom.

5. Conclusions

The Peak Stress Method (PSM) takes advantage of the singular, linear elastic peak stresses calculated at the notch tip by means of FE analyses with coarse meshes to rapidly estimate the mode I, mode II and mode III NSIFs. To this aim, three calibration parameters are required, i.e. K^*_{FE}, K^{**}_{FE} and K^{***}_{FE}. Originally, the PSM was calibrated by using 2D or 3D brick elements, the latter typically requiring a submodel to fulfil the requirements of the mesh pattern dictated by the PSM. To overcome this problem, the PSM has been recently calibrated by using ten-node tetra elements, which are able to discretize complex 3D geometries, the generation of submodels being unnecessary. In the present paper, the PSM has been calibrated by analysing several 3D mode I, II and III V-notch problems, adopting either four-node (which had never been calibrated before) and ten-node tetra elements. The following conclusions can be drawn:

- Dealing with four-node tetra elements, under mode I loading the parameter K^*_{FE} is 1.75 ± 22% for all considered notch opening angles; convergence is obtained when the mesh density ratio $a/d \geq 3$. Under mode II loading, the constant K^{**}_{FE} is 2.65 ± 15% for a mesh density ratio $a/d \geq 3$. Under mode III loading, K^{***}_{FE} results 2.50 ± 15% for all considered notch opening angles; convergence occurs when $a/d \geq 5$.
- Concerning ten-node tetra elements, the obtained results are in agreement with previous calibration. The parameters K^*_{FE} and K^{***}_{FE} have slightly been modified to include additional notch opening angles, namely (i) 120° under mode I and (ii) 90° as well as 120° under mode III. Results are summarized in Table 1.
- In summary, for a general mixed mode I+II+III loading at the weld toe and at the weld root, Table 1 highlights that four-node tetra elements require more mesh refinement than ten-node tetra elements, the minimum mesh density ratio being 5 and 3, respectively. However, the number of FE nodes in the two element types makes the four-node tetra element more convenient. It has been verified on an industrial case of a large welded steel structures that the four-node tetra element mesh generates 57% less FE nodes than a ten-node tetra element mesh.
- Finally, FE meshes being coarse and post-processing the calculated peak stresses being relatively rapid and simple, the PSM based on three-dimensional models of tetra elements might be useful in the everyday design practice, even when large-scale and geometrically complex structures are analysed.

6. References

Atzori B, Meneghetti G (2001) Fatigue strength of fillet welded structural steels: finite elements, strain gauges and reality. Int J Fatigue 23:713–721. doi: 10.1016/S0142-1123(01)00028-7

Campagnolo A, Meneghetti G (2018) Rapid estimation of notch stress intensity factors in 3D large-scale welded structures using the peak stress method. MATEC Web Conf. doi: 10.1051/matecconf/201816517004

Colussi M, Berto F, Meneghetti G (2017), in: P. Bailey, F. Berto, E.R. Cawte, P. Roberts, M.T. Whittaker, J.R. Yates (Eds.), 7th Int. Conf. Durab. Fatigue - Fatigue 2017, Engineering Integrity Society, Cambridge, UK, 2017: 247–258. .

Gross B, Mendelson A (1972) Plane elastostatic analysis of V-notched plates. Int J Fract Mech 8:267–276. doi: 10.1007/BF00186126

Kihara S, Yoshii A (1991) A Strength Evaluation Method of a Sharply Notched Structure by a New Parameter, "The Equivalent Stress Intensity Factor." JSME Int journal Ser 1, Solid Mech strength Mater 34:70–75. doi: 10.1299/jsmea1988.34.1_70

Lazzarin P, Sonsino CM, Zambardi R (2004) A notch stress intensity approach to assess the multiaxial fatigue strength of welded tube-to-flange joints subjected to combined loadings. Fatigue Fract Eng Mater Struct 27:127–140. doi: 10.1111/j.1460-2695.2004.00733.x

Lazzarin P, Tovo R (1998) A notch intensity factor approach to the stress analysis of welds. Fatigue Fract Eng Mater Struct 21:1089–1103. doi: 10.1046/j.1460-2695.1998.00097.x

Meneghetti G (2012) The use of peak stresses for fatigue strength assessments of welded lap joints and cover plates with toe and root failures. Eng Fract Mech 89:40–51. doi: 10.1016/j.engfracmech.2012.04.007

Meneghetti G (2013) The peak stress method for fatigue strength assessment of tube-to-flange welded joints under torsion loading. Weld World 57:265–275. doi: 10.1007/s40194-013-0022-x

Meneghetti G, Campagnolo A, Avalle M, et al (2018) Rapid evaluation of notch stress intensity factors using the peak stress method: Comparison of commercial finite element codes for a range of mesh patterns. Fatigue Fract Eng Mater Struct. doi: 10.1111/ffe.12751

Meneghetti G, Campagnolo A, Rigon D (2017a) Multiaxial fatigue strength assessment of welded joints using the Peak Stress Method – Part I: Approach and application to aluminium joints. Int J Fatigue 101:328–342. doi: 10.1016/j.ijfatigue.2017.03.038

Meneghetti G, Campagnolo A, Rigon D (2017b) Multiaxial fatigue strength assessment of welded joints using the Peak Stress Method – Part II: Application to structural steel joints. Int J Fatigue 101:343–362. doi: 10.1016/j.ijfatigue.2017.03.039

Meneghetti G, Guzzella C (2014) The peak stress method to estimate the mode I notch stress intensity factor in welded joints using three-dimensional finite element models. Eng Fract Mech 115:154–171. doi: 10.1016/j.engfracmech.2013.11.002

Meneghetti G, Lazzarin P (2007) Significance of the elastic peak stress evaluated by FE analyses at the point of singularity of sharp V-notched components. Fatigue Fract Eng Mater Struct 30:95–106. doi: 10.1111/j.1460-2695.2006.01084.x

Meneghetti G, Lazzarin P (2011) The Peak Stress Method for Fatigue Strength Assessment of welded joints with weld toe or weld root failures. Weld World 55:22–29. doi: 10.1007/BF03321304

Qian J, Hasebe N (1997) Property of eigenvalues and eigenfunctions for an interface V-notch in antiplane elasticity. Eng Fract Mech 56:729–734. doi: 10.1016/S0013-7944(97)00004-0

Williams ML (1952) Stress singularities resulting from various boundary conditions in angular corners of plates in tension. J Appl Mech 19:526–528.